Confined photon modes with triangular symmetry in hexagonal microcavities in 2D photonic Crystals

Yuriy A. Kosevich* and José Sánchez-Dehesa†

Wave Phenomena Group, Department of Electronic Engineering,

Polytechnic University of Valencia, c/Camino de Vera s/n, E-46022 Valencia, Spain

Alfonso R. Alija, Luis J. Martínez, Maria L. Dotor and Pablo A. Postigo

Instituto de Microelectrónica de Madrid,

Centro Nacional de Microelectrónica,

Consejo Superior de Investigacion Cientificas,

Isaac Newton 8, PTM Tres Cantos, 28760 Madrid, Spain

Dolores Golmayo

Instituto de Ciencia de Materiales,

Consejo Superior de Investigacion Científicas, Cantoblanco, 28049 Madrid, Spain

(Dated: March 20, 2007)

Abstract

We present theoretical and experimental studies of the size and thickness dependencies of the optical emission spectra from microcavities with hexagonal shape in films of two-dimensional photonic crystal. A semiclassical plane-wave model, which takes into account the electrodynamic properties of quasi-2D planar photonic microcavity, is developed to predict the eigenfrequencies of the confined photon modes as a function of both the hexagon-cavity size and the film thickness. Modes with two different symmetries, triangular and hexagonal, are critically analyzed. It is shown that the model of confined photon modes with triangular symmetry gives a better agreement between the predicted eigenmodes and the observed resonances.

PACS numbers: 42.70.QS, 78.55.-m, 42.25.Fx, 87.64.Xx

I. INTRODUCTION

New physics often emerges in confined systems when reduced dimensionality leads to new symmetries that, together with the confinement, result in new interesting phenomena. Microcavities in two-dimensional photonic crystals (2D PhCs) are an important example of actual confining structures. They are used for localization of photons into PhC bandgaps (BGs) in order to build ultra-small, low-loss, low-power and low-threshold lasers and light-emitting structures[1]. In recent years an important amount of research, both fundamental and applied, has been focused on PhCs microcavities with hexagonal shape fabricated in semiconductor slabs perforated with holes, see, e.g.,[2,3], the vertical emission and lasing from which have been successfully demonstrated[4,5,6]. In such microcavities, light waves having frequencies inside the photonic bandgap are trapped and develop confined photon modes, some of them can be considered as circulating around the perimeter of the cavity due to multiple total internal reflections at its boundary (whispering gallery-type modes)[7,8]. Vertical emission and lasing from such microcavities can be achieved by the coupling of the confined phonon modes (with TE polarization) to the vacuum states. Similar "vertically emitting" 2D systems are also realized in live nature, for example in fluorescent butterfly wing scales[9].

The eigenfrequencies of the confined photon modes are among most important characteristics of a microcavity: they determine the energies of photons having maximal spontaneous emission probabilities (the Purcell effect). In this work we present both theoretical and experimental arguments in favor of the existence of two degenerate photon eigenmodes with *triangular symmetry* in hexagonal microcavities. A semiclassical plane-wave model, which takes into consideration electrodynamic properties of quasi-2D planar photonic microcavity, is developed to predict the eigenfrequencies of the confined photon modes as a function both of the hexagon-cavity size and film thickness. We show that the eigenfrequencies of the triangular-symmetry modes determine spectral positions of spontaneous emission peaks, which were recently observed in photoluminescence spectra from microcavities in a 2D PhC in III-V semiconductor slabs [10]. Here, a new set of microcavities has been built and characterized. As in Ref. [10], by accurate changing the PhC film thickness the wavelengths of the PhC microcavity eigenmodes are tuned in order of tens of nanometers toward higher energies. A comparison of the observed eigenmodes with the spectral positions predicted by the

models of the modes with triangular symmetry and hexagonal symmetry has also been performed. From that comparison we conclude that the proposed model of triangular-symmetry modes gives better agreement with the experiment than that based on hexagonal-symmetry modes. Therefore we expect that the proposed model of triangular-symmetry modes will be useful both in understanding the physical origin and for the quantitative prediction of the spontaneous emission peaks in 2D PhC microcavities in the form of ideal and distorted hexagons.

II. EXPERIMENTAL SETUP

Experimentally, several 2D PhC structures with a hexagonal lattice of circular air holes have been fabricated in an InGaAsP semiconductor film incorporating an active medium composed of three $In_{0.47}Ga_{0.53}As$ quantum wells. This structure gives rise to strong photoluminescence (PL) spectra centered around 1500 nm at room temperature. Processing of the PhC structures was done by electron-beam lithography of a poly(methyl methacrylate) (PMMA) layer on top of a SiO_2 layer (120 nm thick)[10]. To provide the membranes with sufficiently strong mechanical support, the fabricated layers were bonded to a thin borosilicate glass ($n = 1.53$) with optical glue ($n = 1.5$). Circular holes were made in the InGaAsP membrane by reactive ion beam etching. A 2D hexagonal PhC array with lattice constant $a = 500$ nm surrounds hexagonal microcavities with a variable number of missing holes per side. Here, H3 (three missing holes per side) and H5 (three missing holes per side) microcavities are fabricated and characterized. Figure 1 shows a scanning electron microscopy image of one H5 microcavity and a descriptive drawing of the fabricated structure. Different values of the radius of the holes r around $0.33a$ have been used. The variation of the radius r is estimated from the scanning electron microscopy pictures, being below 5%. With this choice of parameters, a large band gap exists for the TE mode between the normalized frequencies of $\omega a/(2\pi c) \sim 0.28$ and $\omega a/(2\pi c) \sim 0.36$, which corresponds to the wavelength range of 1250-1600 nm. The fabricated structures are optically pumped with a 780 nm laser diode. An objective lens (0.40 NA) is used to focus the excitation spot. The size of the excitation spot was around 3.5 μm which is small enough to fit inside the PC structures and to generate cavity modes. Light is collected by a lens inside a 0.22 m monochromator with a cooled InGaAs photodiode connected to a lock-in amplifier. The resolution of the

experimental setup in this configuration is around 2.5 nm.

III. MODEL

Now we turn to the description of our model. Figure 2(a) shows the hexagonal cavity and the ray paths, which belong to the two degenerate triangular-symmetry modes. Within the semiclassical plane-wave model, the dispersion equation for the degenerate triangular-symmetry photon modes, confined in an ideal hexagonal microcavity in 2D PhC, can be obtained from the requirement that the total phase shift of the wave along its closed path is an integer multiple of 2π:

$$k_i^{(N)} 4.5R - 3\phi = 2\pi N, \tag{1}$$

$$\frac{\omega_N}{2\pi} = \frac{c_i}{\lambda_i^{(N)}} = \frac{c}{4.5Rn_{eff}}(N + \frac{3\phi}{2\pi}), \tag{2}$$

where N is integer "quantum" wavenumber, ϕ takes into account the additional phase shift that occurs during the total internal reflection of the confined photon mode in the 2D PhC bandgap frequency region, c_i and $k_i = 2\pi/\lambda_i$ are, respectively, the wave velocity and the *in-plane* wave-vector inside the cavity. It will be shown below that the corresponding wavenumbers N in the considered H3 and H5 microcavities are rather large, $N \gg 1$, which justifies the use of the semiclassical plane-wave model in resolving the eigenfrequencies.

We assume that in (or close to) the middle of the PhC bandgap the additional phase shift ϕ in Eqs. (1) and (2) is equal to the Keller additional phase shift due to leakage of (electron) wavefunction into classically forbidden regions, $\phi = \frac{\pi}{2}$, see Refs. [11]. In the middle of the PhC BG, the phase shift 3ϕ does not depend on the exact form and steepness of the effective confining potential, is independent of wavenumber N and depends only on the number of turning points (equal to 3 or 6 for the triangular- or hexagonal-symmetry modes, respectively, see Figs. 2(a) and 2(b)). It is worth mentioning that we assume that in the middle of the BG the additional phase shift $\phi = \frac{\pi}{2}$ in Eqs. (1) and (2) is fixed and does not explicitly depend on the phase of the coefficient of the total internal reflection of the confined photon modes, in contrast to the similar to Eqs. (1) and (2) semiclassical plane-wave model which was applied to the total-internal-reflection dielectric microresonators with hexagonal cross section, see Ref. [12]. The point is that the phase of the coefficient of the total internal reflection is different (and the difference is equal to π) for the reflection

coefficients of the **E** or **H** fields, which results in different signs of the normal component of the Pointing vector, $\mathbf{P} = \frac{c}{4\pi}\mathbf{E}\times\mathbf{H}$, for the incident and reflected electromagnetic waves, see, e.g., Ref. [13]. Therefore with our choice of ϕ in Eqs. (1) and (2), the wavenumber N is uniquely defined, as in the case of semiclassical Bohr-Sommerfeld quantization condition for the bound electron motion. If we apply the same model to the hexagonal-symmetry photon mode, confined in 2D PhC hexagonal microcavity (in the middle of the PhC BG), see Fig. 2(b), $4.5R$ and 3ϕ in l.h.s. of Eq. (1) and r.h.s. of Eq. (2) should be replaced, respectively, by $3\sqrt{3}R$ and 6ϕ, with $\phi = \frac{\pi}{2}$.

The degeneracy of the two triangular-symmetry modes in an ideal hexagonal microcavity can be removed in a "distorted hexagon", which is bound by two regular triangles with different sides (see Fig. 2(c)). In this case the total optical paths and correspondingly the eigenfrequencies of the two modes, bound inside the different triangles, will be different.

The cavity eigenfrequencies ω_N in Eq. (2) are determined by the effective refractive index of the system $n_{eff} \equiv c/c_i$. The n_{eff} is determined in turn by electrodynamic properties of quasi-2D planar photonic microcavity. The approach of the effective refractive index allows us to describe the actual 3D system as an effective 2D system, see also Ref. [14]. The n_{eff} depends on the polarization of the confined photon mode (TE or TM), and on the relative film thickness $k_i d/2\pi = d/\lambda_i$ of the quasi-2D planar structure. It is possible to obtain an explicit dependence n_{eff}=$n_{eff}(d/\lambda_i)$ by solving dispersion equation for electromagnetic mode in a waveguide formed by a dielectric film with thickness d and dielectric constant ϵ_f, sandwiched between a substrate and a top with dielectric constants ϵ_s and ϵ_t, respectively, see, e.g., Ref. [15]. The dispersion equation for the angular frequency ω of TE mode with a given in-plane wave vector k_i in such planar waveguide system has the following form[15]:

$$\begin{aligned} \tan\kappa_f d &= \frac{(\kappa_t+\kappa_s)\kappa_f}{\kappa_f^2-\kappa_t\kappa_s}, \\ \kappa_f &= \sqrt{\frac{\omega^2}{c^2}\epsilon_f - k_i^2}, \quad \kappa_{t,s} = \sqrt{k_i^2 - \frac{\omega^2}{c^2}\epsilon_{t,s}}. \end{aligned} \tag{3}$$

Equation (3) can be cast in the following transcendent equation which relates ϵ_{eff}=n_{eff}^2, ϵ_f>ϵ_{eff}>(ϵ_t,ϵ_s), with the dimensionless in-plane wavenumber $k_i d$:

$$\tan\left[k_i d\sqrt{\frac{\epsilon_f}{\epsilon_{eff}}-1}\right] =$$

$$\frac{\left[\sqrt{1-\frac{\epsilon_s}{\epsilon_{eff}}}+\sqrt{1-\frac{\epsilon_t}{\epsilon_{eff}}}\right]\sqrt{\frac{\epsilon_f}{\epsilon_{eff}}-1}}{\frac{\epsilon_f}{\epsilon_{eff}}-1-\sqrt{1-\frac{\epsilon_s}{\epsilon_{eff}}}\sqrt{1-\frac{\epsilon_t}{\epsilon_{eff}}}}. \tag{4}$$

Figure 3 presents a numerical solution of Eq. (4) for the TE_0 mode for n_{eff} as a function of d/λ_i (in the interval of interest for our microcavities) in a InGaAsP planar waveguide bonded on a SiO_2 substrate, and using air as top layer. Figure 3 shows that n_{eff} is a monotonously increasing function of d/λ_i, which can be explained by the stronger confinement inside the high-index InP layer of the cavity modes with the smaller, with respect to the layer thickness, wavelengths. Qualitatively similar dependence of n_{eff} on d in a 2D PhC system was previously obtained in Ref. [16] by numerical evaluation of the space-averaged electric-field mode energy.

IV. RESULTS AND DISCUSSION

The d/λ_i-dependence of n_{eff} in Eq. (2) furnishes the clue to a quantitative description within the proposed model of the observed d-dependence of the microcavity eigenfrequencies. To describe the predicted eigenfrequencies (emission peaks) in the measured optical spectra, see Fig. 4, we use $R = 5a$ and $R = 3a$ as the side lengths of the H5 and H3 microcavities in Eqs. (1) and (2). Symbols in Fig. 5 show the spectral positions of the observed absolute eigenfrequencies (in reduced units), $\omega_N a/2\pi c$, as a function of the InGaAsP film thickness (d), while solid (dashed) lines give the predicted by Eqs. (1) - (4) eigenfrequencies of the confined triangular-symmetry (hexagonal-symmetry) photon modes, without any fitting parameters.

Within the model of triangular-symmetry modes, $N = 19$, $N = 20$ and $N = 21$ correspond, respectively, to the 1st, 2nd and 3rd peak in the H5 cavity, and $N = 11$ and $N = 12$ correspond to the 1st and 2nd peak in the H3 cavity. (Within the model of hexagonal-symmetry modes, $N_{hex} = 21$, $N_{hex} = 22$ and $N_{hex} = 23$ correspond, respectively, to the 1st, 2nd and 3rd peak in the H5 cavity, and $N_{hex} = 11$ and $N_{hex} = 12$ correspond to the 1st and 2nd peak in the H3 cavity.) The corresponding wavenumbers N (and N_{hex}) are indeed large, as it was mentioned above. The best agreement of the model of triangular-symmetry modes with the measurements is reached for the half-wavelength layer, d =235 nm$\approx \lambda/2n_f$, λ being the vacuum wavelength. In this case the wave path is indeed close to the two-dimensional path in the plane of the microcavity, while the path becomes more three-dimensional for the

larger slab thicknesses. It is seen in Fig. 5 that the model of triangular-symmetry modes describes better the absolute eigenfrequencies of the observed confined modes both in H5 and H3 microcavities.

Figure 6 shows dimensionless eigenfrequencies $\omega a n_{eff}/2\pi c = a/\lambda_i$ with corresponding wavenumbers N and N_{hex} (for the triangular- and hexagonal-symmetry modes, respectively) versus InGaAsP layer thickness. Now, solid (dashed) lines represent the constant values predicted by Eq. (2) for the confined triangular-symmetry (hexagonal-symmetry) modes, and different bold symbols define the peaks in the optical spectra (not shown) measured in a new set of H5 and H3 fabricated microcavities. To include the experimental data in Fig. 6, we have used Eq. (4) [for the same $n_{eff}(d/\lambda_i^{(N)})$ as in Fig. 5].

The agreement found with the new data also supports our model of confined photon modes with triangular symmetry. Another evidence in favor of the proposed semiclassical plane-wave model can be obtained from previously published measurements of photoluminescence spectra from hexagonal microcavities in 2D photonic crystlas. For instance, one can deduce from the spectra in Ref. [17] that the spacing between the strongest photoluminescence peaks in H2 and H5 hexagonal microcavities in 2D PhCs scales with the cavity size R as 1/R. Namely, the spacing between the two strongest neighbor peaks seen in Figs. 2b and 2c of Ref. [17] are approximately equal to 130 and 53 nm for H2 and H5 microcavities, respectively. The ratio of these peak spacings is indeed close to the value 5/2, given by the inverse ratio of the cavity sizes. Another earlier observation, to which we can refer in support of our proposed plane-wave model is the blue shift of spontaneous emission spectra from the suspended 2D PhC microcavities, surrounded from both sides by air, with respect to the spectra from microcavities grown on Si wafer with SiO_2 transfer layer, see Figs. 1 and 8 in Ref. [17]. The effective refractive index n_{eff} of the planar photonic microcavity is lower in the former structure which results in the blue shift of the cavity eigenfrequencies, in accordance with Eq. (2).

In connection with aforementioned comparison between the predicted and observed microcavity photon eigenmodes, it is important to emphasize that the reason why the triangular-symmetry modes give the predominant contribution to photoluminescence spectra in actual heterostructures is possibly related with relatively high *modal volume* of these modes which increases the coupling of these modes to the vacuum states, see, e.g., Ref. [8]. Namely, as follows from the comparison of the ray paths for the triangular- and hexagonal-symmerty

modes in Figs. 2(a) and 2(b), the hexagonal-symmetry modes are confined more close to the cavity boundary and therefore give less contribution to the far-field emission from the cavity, which comes mainly from the "bulk-like" cavity eigenmodes. The same arguments can be applied to the comparison between the emission strengths of the bulk-like trianguar-symmetry modes in hexagonal microcavities and a dense set of cavity eigenmodes, which were predicted for H5 hexagonal microcavities in 2D PhC with the use of finite-difference time-domain simulations in Ref. [8]. As it is explained in Ref. [8], only few of the predicted eigenmodes can emit strong enough far-field radiation, the other eigenmodes have very "spotty patterns" which suppress the emission. It is also worth mentioning in this connection that the possible origin of some of the less strong peaks, in comparison with that given by the triangular-symmetry modes, in the observed photoluminescence spectra [Fig. 2 in Ref. [17]] can be the additional cavity eigenmodes caused by the splitting of the degenerate triangular-symmetry eigenmodes in hexagonal cavities by fabrication imperfections and defects. The splitting of spectrally degenerate cavity modes by unavoidable cavity imperfections was previously observed and studied, see, e.g., Refs. [18,19].

At this point, let us remember that dielectric microresonators and microcavities with hexagonal shape, which are often called as whispering-gallery resonators, have also attracted much interest for possible optical applications in recent years. The whispering-gallery modes in dielectric resonators with hexagonal shape correspond to the hexagonal-symmetry modes in hexagonal microcavities in 2D PhC (see Fig. 2(b)). The "horizontal" emission from such dielectric microresonators is achieved by the coupling of the confined phonon modes with TM polarization to the vacuum states. A semiclassical plane-wave model of triangular-symmetry modes can also be applied to quasi-2D planar dielectric microresonators. Recent studies of dielectric microresonators made of zinc oxide (ZnO) nanoneedles with hexagonal cross section have been reported in Ref. 12. The refractive index n of ZnO is close to 2 and, therefore, the critical angle of incidence for total internal reflection in the microresonator is close to $\pi/6$. Since the angle of incidence of triangular-symmetry (whispering-gallery) modes in hexagonal microresonator is $\pi/6$ ($\pi/3$), see Figs. 2(a) and 2(b), the triangular-symmetry modes in planar, with half-wavelength thickness $d \approx \lambda/2n$, dielectric microresonators made of ZnO can be considered as *radiating* counterparts of *non-radiating* whispering-gallery modes.

V. SUMMARY

In summary, theoretical and experimental evidences have been presented showing that confined double-degenerated photon eigenmodes with triangular symmetry can be the origin of the emission peaks observed in the optical spectra from planar hexagonal microcavities in 2D photonic crystals. Here, an analytical semiclassical plane-wave model, which takes into consideration electrodynamic properties of quasi-2D planar photonic microcavity, has been developed for the quantitative evaluation of the eigenfrequencies of the photon modes, laterally localized due to the total internal reflection in the middle of photonic crystal bandgap. This analytical model describes quantitatively the experimentally observed cavity-size and photonic-crystal-thickness dependencies of the eigenfrequencies of the confined photon modes. Removal of the degeneracy and change of eigenfrequencies of the confined photon modes are predicted for hexagonal microcavities with imperfections and for microcavities in the form of distorted hexagon.

VI. ACKNOWLEDGEMENTS

Work supported by Ministry of Science and Education (MEC) of Spain (Refs. TEC2004-03545, TEC2005-05781-C03-01, NAN2004-08843-C05-04, NAN2004-09109-C04-01), and contracts S-505/ESP/000200, UE NoEs SANDIE (NMP4-CT-2004-500101) and PHOREMOST (IST-2-511616-NOE). The authors acknowledge useful discussions with Andreas Håkansson, Javier Martí and Daniel Torrent. Yu. A. K. acknowledges a support from MEC (Grant SAB2004-0166). A. R. A. thanks a FPU fellowship (Ref. AP2002-0474) and L. J. M. an I3P fellowship.

* Permanent address: Semenov Institute of Chemical Physics, Russian Academy of Sciences, ul. Kosygina 4, 119991 Moscow, Russia. yukosevich@yahoo.com.

† Corresponding author. E-mail:jsdehesa@upvnet.upv.es

[1] For recent reviews see S. Noda, Science, **284**, 1819 (2006); K. Vahala, Nature (London), **432**, 839 (2003).

[2] S. Noda and T. Baba, *Roadmap on Photonic Crystals* (Kluwer Academic Publishers, Dordrecht, 2003).

[3] Jean-Michel Lourtioz, Henri Benisty, Vincent Berger, Jean-Michel Gérard, Daniel Maystre, and Alexis Tchelnokov, *Photonic Crystals: Towards Nanoscale Photonic Devices* (Springer-Verlag, Berlin, 2005).

[4] O. Painter, R.K. Lee, A. Sherer, A. Yariv, J.D. O'Brien, P.D. Dapkus, and I.Kim, Science, **284**, 1819 (1999).

[5] H-G. Park, S.-H. Kim, S.H. Kwon, Y.G. Ju, J.K. Yang, J.H. Baek, S.B. Kim, and Y.H.Lee, Science, **305**, 1444 (2004).

[6] M. Fujita, S. Takahashi, Y. Tanaka, T. Asano, and S. Noda, Science, **308**, 1296 (2005).

[7] P. Pottier, C. Seassal, X. Letartre, J.L. Leclerq, P. Viktorovitch, D. Cassagne, and C. Joannin, J. Lightwave Technol. **17**, 2058 (1999).

[8] H. Benisty, C. Weisbuch, D. Labilloy, M. Rattier, C. J. M. Smith, T. F. Krauss, R. M. De La Rue, R. Houdre, U. Oesterle, C. Jouanin, and D. Cassagne, IEEE J. Lightwave Technol. **17**, 2063 (1999).

[9] P. Vukusic and I. Hooper, Science, **310**, 1151 (2005).

[10] A. R. Alija, L. J. Martinez, A. Garcia-Martin, M. L. Dotor, D. Golmayo, and P. A. Postigo, Appl. Phys. Lett. **86**, 141101 (2005).

[11] J. B. Keller, Ann. Phys. (NY) **4**, 180 (1958); A. D. Stone, Phys. Today **58**, No. 8, 37 (2005).

[12] Th. Nobis, E. M. Kaidashev, A. Rahm, M. Lorenz, and M. Grundmann, Phys. Rev. Lett. **93**, 103903 (2004).

[13] L. D. Landau and E. M. Lifshitz, *Electrodynamics of Continuous Media* (Butterworth-Heinemann, Oxford, 1984).

[14] M. Qiu, Appl. Phys. Lett. **81**, 1163 (2002).

[15] H. A. Haus, *Waves and Fields in Optoelectronics* (Prentice-Hall, New Jersey, 1984).

[16] H. Y. Ryu, J. K. Hwang, and Y. H. Lee, IEEE J. Quantum Electron., **39**, 314 (2003).

[17] C. Monat, C. Seassal, X. Letarte, P. Regreny, M. Gendry, P. Rojo Romeo, P. Viktorovitch, M. Le Vassor d'Yerville, D. Cassagne, J. P. Albert, E. Jalaguier, S. Pocas, and B. Aspar, J. Appl. Phys. **93**, 23 (2003).

[18] O. Painter and K. Srinivasan, Opt. Lett. **27**, 339 (2002).

[19] K. Hennesy, C. Hoegerle, E. Hu, A. Badolato, and A. Imamoglu, Appl. Phys. Lett. **89**, 041118 (2006).

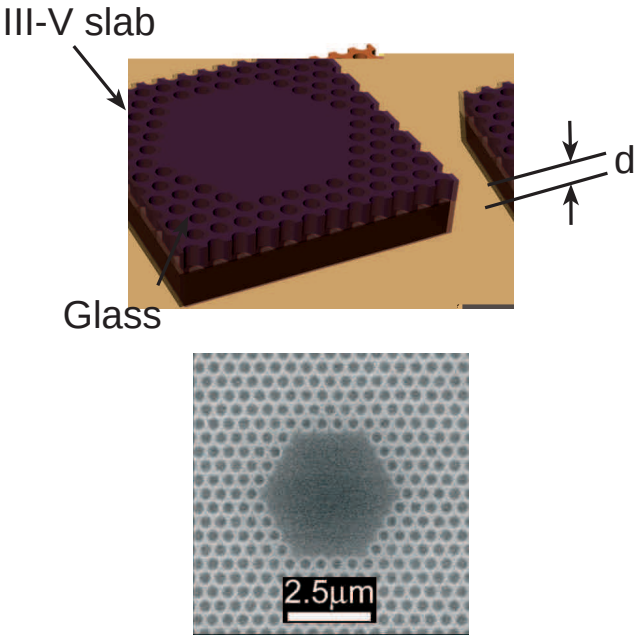

FIG. 1: (Lower image) Scanning electron microscopy image of the fabricated H5 cavities. (Upper image) Schematic view of H5 microcavity fabricated on the III-V semiconductor slab with a thickness d=265 nm bonded to a glass substrate.

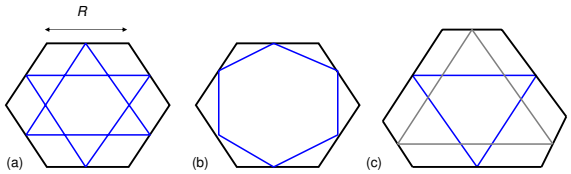

FIG. 2: (color online) Ray paths in triangular-symmetry modes in ideal, (a), and distorted, (c), hexagons; (b) presents ray path for the hexagonal-symmetry mode in an ideal hexagon. Two triangular-symmetry modes are degenerate in an ideal hexagon, and have different optical paths and eigenfrequencies in a distorted hexagon.

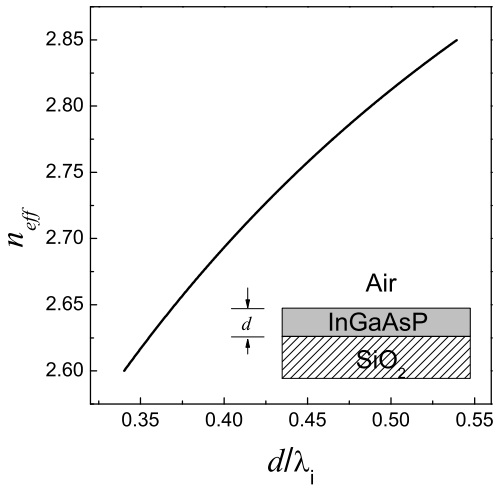

FIG. 3: Effective refractive index n_{eff} versus InGaAsP layer thickness over internal wavelength d/λ_i in a planar waveguide with $\epsilon_f = 10.89$ (InGaAsP), $\epsilon_s = 2.34$ (SiO_2) and $\epsilon_t = 1$ (air).

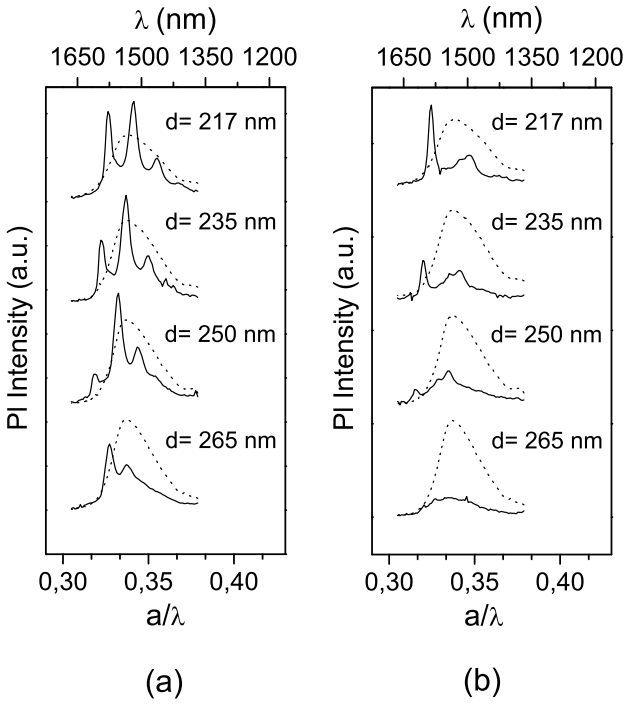

FIG. 4: Photoluminescence spectra of the H5 (a) and H3 (b) microcavities with different slab thicknesses d (solid lines). The spectra of an unpatterned region in the vicinity of the microcavity is also shown (dotted lines). Here λ is the vacuum wavelength: $a/\lambda = \omega a/2\pi c$.

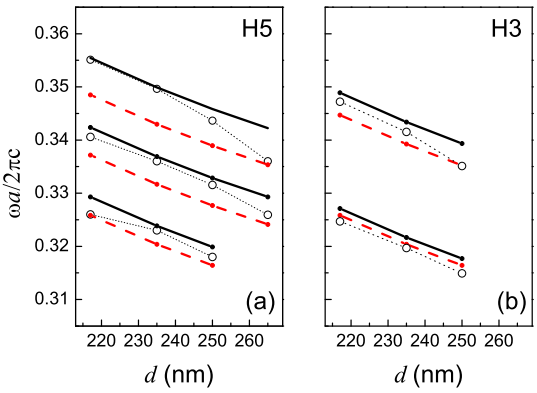

FIG. 5: (color online) Normalized frequencies of emission peaks produced by localized modes in H5 (a) and H3 (b) microcavities as a function of InP layer thickness, d. Open circles represent the experimental data obtained by microphotoluminescence. The dotted lines are guides for the eye. Solid (red dashed) lines show the theoretical prediction given by the model of confined triangular-symmetry (hexagonal-symmetry) modes.

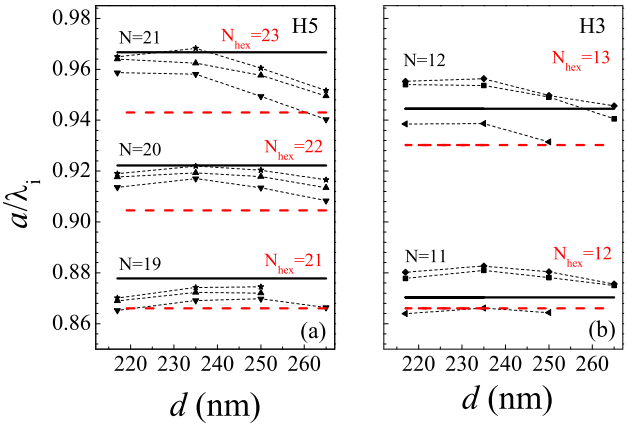

FIG. 6: (color online) Normalized eigenfrequencies with corresponding wavenumbers N and N_{hex} (for the triangular- and hexagonal-symmetry modes, respectively) of emission peaks produced by confined photon modes in H5 (a) and H3 (b) microcavities as a function of InP layer thickness d. Different bold symbols represent the experimental data obtained by microphotoluminescence. Solid (red dashed) lines represent the theoretical prediction given by the model of confined triangular-symmetry (hexagonal-symmetry) modes.